

RARE EARTH AND RELATED ELEMENTS IN THE GOODRICH QUARTZITE, MARQUETTE COUNTY, MICHIGAN

by

B.K. Parker
Geological Survey Division,
Department of Natural Resources,
Lansing, Michigan

1987

Michigan Geological Survey Division
Open File Report OFR 81-2
22 pages, 0 plates

This report is made from the best available copy.

It is a Preliminary, unedited information release, subject to revision.

If this report is formally published it will no longer be available as an Open File Report.

This report is printed by the State of Michigan and may be purchased from:

Geological Survey Division
Michigan Department of Natural Resources
P O Box 30028
Lansing, Michigan 48909

A list of Open File Reports and Maps is also available from the Geological Survey Division upon request.

Reproduction of Michigan Geological Survey Division publications in whole or in part, may be done and is encouraged if proper credit is given to the Michigan Department of Natural Resources, Geological Survey Division and, where appropriate, the author(s).

ABSTRACT

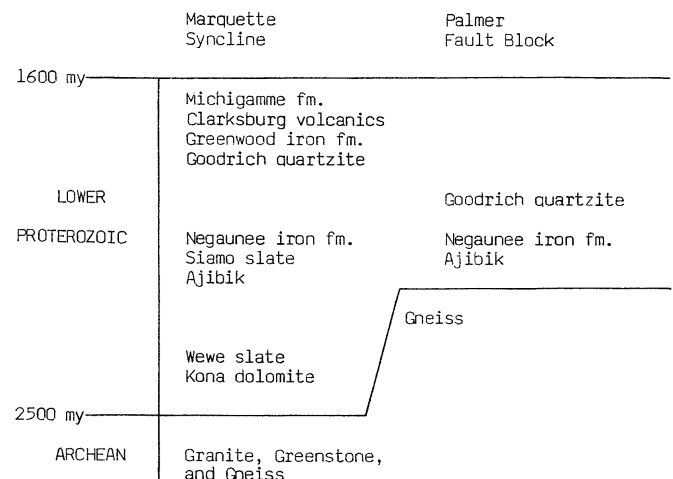
Ten samples of Goodrich quartzite, collected from radioactive outcrops and glacial boulders in the Palmer Area, Marquette County, Michigan, were analyzed for the rare earth elements (REE) lanthanum to lutetium, thorium, and uranium. Precious metals were also analyzed. The rare earth elements, thorium, and uranium correlate very well with each other, indicating: 1) the REE. Th. and U abundance is controlled only by the total amount of detrital monazite present and 2) the composition of the monazite is constant throughout its L square mile area of occurrence. The composition of the monazite can be calculated from the rock abundance of REE because other minerals in the quartzite are shown to be negligible in REE. Normalized REE patterns are highly enriched in light end REE and show a large negative europium anomaly. The consistent composition of the detrital monazite is a good fingerprint for determining the source area of the monazite. If the chemical composition of monazite in a local granite, or

other rock type, matches that of the detrital monazite in the Goodrich, then a likely source area is indicated.

INTRODUCTION

The Palmer area is located approximately 20 miles southwest from Marquette, Michigan. The Precambrian terrain in this region consists of Archean granites, granite-gneisses and greenstones plus lower Proterozoic metasediments and metavolcanics. The metasediments and metavolcanics have been tightly folded to form the major structure in the area, the westward plunging Marquette syncline. The Palmer area occupies about 4 square miles and represents a downfaulted portion of the southern limb of the syncline. Within the fault block of the Palmer area the three main formations are in ascending order, the Ajibik quartzite, the Negaunee iron formation and the Goodrich quartzite. A comparison of the stratigraphy in the Marquette syncline with that in the Palmer fault block is shown in Table 1. Details of geology can be found in Gair (1975); Leith, Lund, and Leith (1975); James (1958); and Vickers (1956).

Table 1
Generalized Stratigraphy - Marquette Syncline and Palmer Fault Block



In 1951 Robert C. Reed, geologist working for L. P. Barrett, U.S. Atomic Energy Commission contractor, discovered anomalous radioactivity near Palmer, Michigan, on rock dumps of Goodrich quartzite near the Old Volunteer and Old Maitland iron mines. R. C. Vickers (1956) reported the radioactivity as due to thorium found in detrital grains of the mineral monazite. (Ce, La, Nd, Th) (PO₄). Vickers conducted detailed mapping of the Goodrich in the Palmer area and logged by gamma-ray technique three existing diamond drill holes. The gamma ray logging indicated most of the monazite is located more than 300 feet above the base of the Goodrich. Although monazite is more abundant in the upper part of the section, exposures of Goodrich are limited to the lower 200 feet of the formation. Spectrographs analyses of monazite concentrates made from outcrop samples provided a semiquantitative look at the REE makeup of the monazite.

Gair (1975) measured the thorium content of outcrops in the Palmer area and calculated a resource of 169,500 tons of inferred thorium, most of it more than 300 feet above the base of the Goodrich.

This report describes the results of 10 samples of Goodrich analyzed for the REE, thorium, uranium, and precious metals. Those elements determined are shown in Table 2.

SAMPLING

Samples of Goodrich quartzite were collected in two general areas. One in the Palmer fault block and another in a glacial boulder field of Goodrich quartzite located 3.5 miles southwest of the Palmer area in NW-NW-Section 2-T46N-R27W (see Map A). Map A shows the general location of these two areas in relation to the eastern part of the Marquette trough. Map B and Map C show sample locations in the Palmer basin and the location of the boulder field, respectively.

Approximately 0.5-1 kilogram of chip sample was collected at each sample location. The samples collected represent the areas of highest radioactivity at a given outcrop, and are not representative of the outcrop area as a whole. Quartzite samples rich in monazite allow a determination of the REE composition of the monazite without using special methods of separating the monazite from the other minerals in the quartzite. Using a whole rock REE analysis to represent the REE pattern of monazite is valid only if the REE abundance in the other minerals of the rock is very low compared to the REE abundance in monazite. This is shown to be the case in a later paragraph.

PETROGRAPHY OF SAMPLES

Thin sections of the 10 Goodrich samples chemically analyzed show a lithology similar to the quartz pebble conglomerate described by Gair (1975). Grains smaller than pebble size are dominated by angular to subrounded Quartz with minor microcline often partly altered to sericite and chlorite. The matrix is dominated by sericite and grains of quartz. Monazite occurs in the matrix as rounded fine to very fine sand size grains. Monazite is also a common inclusion in the quartz grains. Sample GP-18, collected in the SW.SW. Sec. 29. T47N. R26W. differs from the other nine samples because it contains chloritoid, which appears to be pseudomorphous after angular plagioclase grains (albite twinning seems to be present). This occurrence of detrital chloritoid in the Goodrich is in addition to the occurrence in the center of Sec. 29 as mentioned by Gair (1975).

RESULTS

All analyses were done by neutron activation. Elements determined were the REE, U, Th, Sc, and Au. The

abundance of these elements in 10 Goodrich samples are shown in Table 3. As expected, those samples with highest monazite content are the most radioactive and yield the highest REE values. Ce is the most abundant REE and has a range of 5050 ppm to 950 ppm. In abundance Ce is followed by La (2825-490 ppm), Th (2300-450 ppm), and Nd (1500-250 ppm). The maximum for all the other REE is less than 500 ppm.

The rare earth elements La to Ho (57-67) plus Th and U (90 and 92) show a high degree of correlation with each other. All element pairs in this group have correlation coefficients greater than 0.80 with many showing correlation coefficients greater than 0.90. Of the 55 possible pairs within this group 14 have a correlation coefficient greater than 0.99. Some examples are shown in Figures 1 and 2.

The heavier REE. Er, Tm, Yb, and Lu in general show moderate correlation coefficients (0.898-0.478) with the lighter REE elements. Among themselves the correlation coefficient is high for Er vs. Tm (0.968) and Yb vs. Lu (0.938) but low (0.366-.48) for the other possible pairs.

The normalized REE patterns are shown in Figure 3. The average chondrite composition of Haskin et al (1968) was used for all REE except Dy (Schmidt et al; 1963, 1964). The REE pattern is highly enriched in the light end REE, and shows a strong negative Eu anomaly, a slight negative Er anomaly, and slight positive Tm anomaly.

DISCUSSION

Factors affecting the abundance of REE in the quartzite are the total amount of monazite present, REE composition of the monazite, and the amount of other minerals present. The high degree of correlation of the REE elements among themselves indicates monazite is the mineral controlling total REE abundance. The high degree of correlation also indicates the monazite has a very consistent composition. One can then visualize the REE abundance in the Goodrich as due to a mechanical mixture of monazite grains of constant composition with grains of other minerals containing negligible REE. As the monazite content of the mixture varies, the ratio between two REE in the mixture remains the same; but the total amount of the two REE varies in direct proportion to the amount of monazite present. Analyses of two REE in mixtures containing varying amounts monazite would show a linear fit when one REE is plotted against another.

REE in the four samples from glacial boulders in NW NW Section 2, T46N, R27W correlate in the same manner as REE in Goodrich outcrops in the Palmer area. Therefore the monazite in the quartzite glacial boulders is the same composition as monazite in the Palmer area. This leaves little doubt the quartzite glacial boulders in Section 2, T46N, R27W are from the Goodrich formation in the Palmer area, especially since

monazite has not been found in any abundance in Goodrich outcrops outside of the Palmer basin. The length and direction of glacial transport from the Palmer area is about 3 miles to the southwest.

Muscovite and K-feldspar are two minerals present in the quartzite which may contribute to the amount of REE present. Yet these two minerals apparently do not contribute significantly to the total abundance. Using typical values of REE elements found in mica and feldspar (Graf, 1977), a mass calculation indicates the contribution to the total REE abundance from mica and feldspar is minor compared to the contribution from monazite. Exceptions may be Eu, Tb, and Lu. These elements are low enough in concentration that a significant amount of their total abundance may be due to contributions from mica and feldspar. But monazite still exhibits dominant control. Eu which is particularly depleted compared to other REE (see Figure 3), still correlates well with Ce, La, and Pr, indicating control by monazite (Figure 4). Finally, Vickers (1956) used alpha-sensitive stripping on thin sections of the quartzite and determined that almost all the radioactivity is due to monazite.

U correlates well with Ce, La, No (Figure 5), and most of the other REE; indicating monazite also controls the amount of U present. All of the correlation lines converge on the intercept of 10 ppm U when no La, Ce, or Nd is present (i.e. no monazite is present) as shown in Figure 5. This indicates the Goodrich contains two types of U. The first type is background U at 10 ppm. The second type is U found only in monazite. The possibility also exists that the 10 ppm of "background U" is due to background in the counting instrumentation. That is, when no U was actually present, the counting instrument gave a reading of 10 ppm.

The composition of the mineral monazite can be estimated by calculation once the following assumptions are made:

- 1) the mineral is free of Yttrium (element no. 39). Deer, et al (1962) give three analyses of monazite with Yttrium oxide (Y_2O_3) having an abundance of 4-5 weight %.
- 2) the mineral is free of calcium, iron and silica. Deer et al, state that silica is usually present in small amounts and the substitution $Si^{+4} Th^{+4} \rightleftharpoons Ce^{+3}, P^{+5}$ occurs under these conditions.

The calculated composition of the monazite, using the two assumptions above, is shown in Table 4. The assumptions should only introduce minor errors in the calculated composition. As a comparison Vickers (1956) gives two chemical analyses of monazite concentrates. His values for ThO_2 and U_3O_8 can be extrapolated for the concentration expected in pure monazite. The resulting percentages of 11.5% ThO_2 and 0.31% U_3O_8 agree well with the corresponding calculated percentages of 12.2% and 0.30% shown in Table 4.

Conclusions

The high correlations between REE pairs indicates the detrital monazite located in the lower part of the Goodrich quartzite has a consistent composition throughout the 4 square miles of the Palmer fault block. Monazite located more than 200 above the base of the Goodrich was not sampled because this part of the formation is not exposed. The calculated content of ThO_2 and U_3O_8 in the monazite is 12.2% and 0.30% respectively. These percentages also represent the upper limit of ThO_2 and U_3O_8 in a Goodrich heavy mineral placer. Under these unlikely conditions, the heavy mineral placer would consist of only monazite. An exception to this limit could exist if the composition of the monazite becomes richer in ThO_2 and U_3O_8 higher in the stratigraphic section of the Goodrich.

The consistent composition of the monazite is a good "fingerprint" for determining the source area of the monazite. If the chemical composition of monazite in a local pegmatite or granite matches that of the monazite in the Goodrich, then a likely source area is indicated.

REFERENCES

- Deer, Howie, and Zussman
1962: Rock Forming Minerals. Volume 5, Nonsilicates. Longman, London. 371p.
- Gair, J. E.
1975: Bedrock geology and ore deposits of the Palmer Quadrangle, Marquette County, Michigan. U.S. Geological Survey Professional Paper 769, 159p.
- Graf, J. L.
1977: Rare earth elements as hydrothermal tracers during formation of massive sulphide deposits in volcanic rocks. Econ. Geol. Vol. 72, p. 527.
- Haskin, Haskin, Frey, and Wildeman
1968: Relative and absolute terrestrial abundances of the rare earths. In L. H. Ahrens, ed., Origin and Distribution of the Elements, Pergamon Press, New York, p. 889-912.
- James, H. L.
1958: Stratigraphy of pre-Keweenawan rocks in parts of northern Michigan. U.S. Geological Survey Professional Paper 314-C, pp. 27-44.
- Leith, C. K., Lund, R. J., and Leith, A.
1935: Pre-Cambrian rocks of the Lake Superior Region. U.S. Geological Survey Professional Paper 184, 34p.
- Schmitt, Smith, Lasch, Mosen, Olehy, and Vasilevski's
1963: Abundances of the fourteen rare-earth elements, scandium, and yttrium in meteoritic and terrestrial matter, Geochim. Cosmochim. Acta, vol. 27, 577-622.
- Schmitt, Smith, and Olehy
1964: Rare-earth, yttrium, and scandium abundances in meteoritic and terrestrial matter-II, Geochim. Cosmochim. Acta, vol. 28, 67-86.
- Vickers, R. C.
1956: Geology and monazite content of the Goodrich Quartzite, Palmer area, Marquette County, Michigan. U.S. Geological Survey Bulletin 1030-F, p. 171-185.

APPENDIX

Table 2
Rare Earth and Related Elements Determined in 10 Samples of Goodrich Quartzite.

Atomic No.	Symbol	Element	Atomic No.	Symbol	Element
57	La	Lanthanum	68	Er	Erbium
58	Ce	Cerium	69	Tm	Thulium
59	Pr	Praseodymium	70	Yb	Ytterbium
60	Nd	Neodymium	71	Lu	Luteium
62	Sm	Samarium			
63	Eu	Europium			
64	Gd	Gadolinium	Related Elements:		
65	Tb	Terbium	21	Sc	Scandium
66	Dy	Dysprosium	90	Th	Thorium
67	Ho	Holmium	92	U	Uranium

*Au was determined in 9 samples.

Pt and Pd were undetected (Pt less than 15 ppb, Pd less than 300 ppb)

Table 3
Rare Earth Elements, Thorium, Uranium and Precious Metal Analyses of Goodrich Quartzite, Palmer Area

All values in ppm except Au = ppb

Element No.	Symbol	GP-1	GP-3*	GP-5	GP-6*	GP-10*	GP-12	GP-13	GP-17*	GP-18	GP-21
57	La	2,150	2,825	1,300	1,210	1,120	590	2,520	1,550	490	1,480
58	Ce	3,590	5,050	2,250	2,350	2,000	1,100	4,900	2,900	950	2,900
59	Pr	450	550	150	200	150	50	350	200	50	200
60	Nd	1,150	1,900	750	650	600	320	1,350	850	250	800
62	Sm	250	332	160	136	126	68	292	184	60	166
63	Eu	3.2	4.5	2.3	1.8	1.6	1.2	2.7	1.8	1.1	1.8
64	Gd	220	320	80	190	30	30	250	260	10	80
65	Tb	30	30	12	12	11	8	30	14	2	16
66	Dy	90	120	60	50	50	30	110	70	30	60
67	Ho	15	24	12	9	9	7	19	14	8	12
68	Er	25	20	6	6	10	5	11	7	2	7
69	Tm	15	13	3	6	7	3	5	5	2	4
70	Yb	6	15	7	6	5	6	9	6	6	5
71	Lu	0.5	1.9	0.8	0.5	0.8	1.0	0.7	0.6	0.7	0.7
90	Th	1,850	2,300	1,100	1,000	900	500	2,100	1,300	450	1,200
92	U	55	58	37	38	27	18	62	47	20	41
21	Sc	6	12	4	6	6	5	6	21	6	6
79	**Au	99	20	21	21	24	14	10	40	ns	31

Not detected: Pd, Pt; Pd less than 15 ppb, Pt less than 300 ppb
All analyses by neutron activation, Au, Pt, Pr, by fire assay, preconcentration
Analyses by X-Ray Assay Laboratories, Don Mills, Ontario
* Sample from glacial boulder field in NW-1/4-sec. 2-T46N-R27W
** Au in ppb.

Table 4
Calculated Composition of the Detrital Monazite in the Goodrich Quartzite, Palmer Area, Marquette County, Michigan

Oxide	Weight %	Ion composition on basis of 4 (PO ₄)
P ₂ O ₅	29.6	PO ₄ ³⁻ 4.00
Ce ₂ O ₃	28.1	Ce ³⁺ 1.66
La ₂ O ₃	15.1	La ³⁺ .90
Nd ₂ O ₃	8.1	Nd ³⁺ .47
ThO ₂	12.2	Th ⁴⁺ .45
Pr ₂ O ₃	2.3	Pr ³⁺ .14
Sm ₂ O ₃	1.7	Sm ³⁺ .096
Gd ₂ O ₃	1.5	Gd ³⁺ .078
EuO...*	1.10	Eu...** .06+
U ₃ O ₈	0.30	U ⁶⁺ .010
Total	100.00	Total 0

(by calculation)

EuO...* =	EuO,	Tb ₂ O ₃ ,	Dy ₂ O ₃ ,	Ho ₂ O ₃ ,	Er ₂ O ₃ ,	Tm ₂ O ₃ ,
	percent.	Lu ₂ O ₃ ,	1.10 wt%	represents	an	average

Eu...** = Eu²⁺, Tb³⁺, Dy³⁺, Ho³⁺, Er³⁺, Tm³⁺, Yb³⁺, Lu³⁺

semiquantitative chemical composition of the mineral Monazite. Values are calculated from the REE composition of the quartzite. Contributions to total REE abundance from minerals other than monazite is negligible (see text). The calculated composition assumes the Monazite contains no Y, Ca, Fe, or Si. These elements are usually present in only small amounts (Deer et al, 1961). The value shown for wt% U₃O₈ has been corrected for the 10 ppm background uranium found elsewhere in the Goodrich quartzite. Therefore, the amount of wt% U₃O₈ shown is that contained only in Monazite.

CORRELATION COEFFICIENTS
NO. OF SAMPLES = 10*

	CE	LA	TH	ND	PR	SM
CE	1.0000	0.9957	0.9947	0.9936	0.9346	0.9916
LA	0.9957	1.0000	0.9986	0.9989	0.9514	0.9987
TH	0.9947	0.9986	1.0000	0.9978	0.9536	0.9984
ND	0.9936	0.9989	0.9978	1.0000	0.9436	0.9988
PR	0.9346	0.9514	0.9536	0.9436	1.0000	0.9492
SM	0.9916	0.9987	0.9984	0.9988	0.9492	1.0000
GD	0.8860	0.8793	0.8832	0.8778	0.8338	0.8814
DY	0.9887	0.9948	0.9951	0.9948	0.9368	0.9972
U	0.9694	0.9594	0.9653	0.9628	0.8864	0.9579
TB	0.9889	0.9752	0.9694	0.9735	0.8934	0.9698
HO	0.9444	0.9585	0.9548	0.9570	0.9052	0.9668
ER	0.7444	0.7737	0.7856	0.7658	0.8977	0.7705
TM	0.6629	0.6976	0.7052	0.6846	0.8663	0.6918
YB	0.6847	0.7179	0.7053	0.7108	0.7218	0.7333
EU	0.8788	0.9139	0.9131	0.9125	0.9586	0.9224
LU	0.5816	0.6201	0.5954	0.6148	0.5965	0.6318
SO	-0.2145	-0.2040	-0.1996	-0.2317	-0.0844	-0.1929
AU	0.0016	0.0159	0.0325	0.0194	0.1258	0.0157

* No. of samples analyzed for Au = 9

CORRELATION COEFFICIENTS (continued)
NO. OF SAMPLES = 10*

	GD	DY	U	TB	HO	ER
CE	0.8860	0.9887	0.9694	0.9809	0.9444	0.7444
LA	0.8793	0.9948	0.9594	0.9752	0.9585	0.7737
TH	0.8832	0.9951	0.9653	0.9694	0.9548	0.7856
ND	0.8778	0.9940	0.9628	0.9735	0.9570	0.7650
PR	0.8338	0.9368	0.8864	0.8934	0.9052	0.8977
SM	0.8814	0.9972	0.9579	0.9698	0.9668	0.7705
GD	1.0000	0.8808	0.9154	0.8432	0.8533	0.6042
DY	0.8808	1.0000	0.9508	0.9696	0.9729	0.7532
U	0.9154	0.9508	1.000	0.9194	0.8982	0.6938
TB	0.8432	0.9696	0.9194	1.0000	0.9294	0.6943
HO	0.8533	0.9729	0.8902	0.9294	1.0000	0.6826
ER	0.6042	0.7532	0.6938	0.6943	0.6826	1.0000
TM	0.5885	0.6685	0.6139	0.5988	0.6090	0.9683
YB	0.6467	0.7465	0.5606	0.7198	0.8470	0.4801
EU	0.7641	0.9113	0.8113	0.8574	0.9202	0.8368
LU	0.4775	0.6456	0.4150	0.6509	0.7654	0.3861
SC	-0.1789	-0.1599	-0.2672	-0.2777	-0.0214	-0.1392
AU	0.0960	0.0180	0.1567	0.1849	0.0355	0.2967

* No. of samples analyzed for Au = 9

CORRELATION COEFFICIENTS (continued)
NO. OF SAMPLES = 10*

	TM	YB	EU	LU	SC	AU *
CE	0.6629	0.6847	0.8788	0.5816	-0.2145	0.0016
LA	0.6976	0.7179	0.9139	0.6201	-0.2040	0.0159
TH	0.7052	0.7053	0.9131	0.5954	-0.1996	0.0325
ND	0.6846	0.7103	0.9125	0.6140	-0.2317	0.0194
PR	0.8663	0.7218	0.9580	0.9565	-0.0844	0.1258
SM	0.6918	0.7333	0.9224	0.6318	-0.1929	0.0157
GD	0.5885	0.6467	0.7641	0.4775	-0.1789	0.0960
DY	0.6685	0.7465	0.9113	0.6456	-0.1599	0.0180
U	0.6139	0.5606	0.8113	0.4150	-0.2672	0.1567
TB	0.5988	0.7198	0.8574	0.6509	-0.2777	0.1849
HO	0.6090	0.8470	0.9202	0.7654	-0.0214	0.0355
ER	0.9683	0.4801	0.8368	0.3861	-0.1392	0.2967
TM	1.0000	0.4663	0.7993	0.3661	-0.0651	0.3136
YB	0.4663	1.0000	0.8361	0.9382	0.2183	-0.3555
EU	0.7993	0.8361	1.0000	0.7293	-0.0502	0.0001
LU	0.3661	0.9382	0.7293	1.0000	0.1539	-0.3813
SC	-0.0651	0.2183	-0.0502	0.1539	1.0000	-0.0271
AU	0.3136	-0.3555	0.0001	-0.3813	-0.0271	1.0000

* No. of samples analyzed for Au = 9

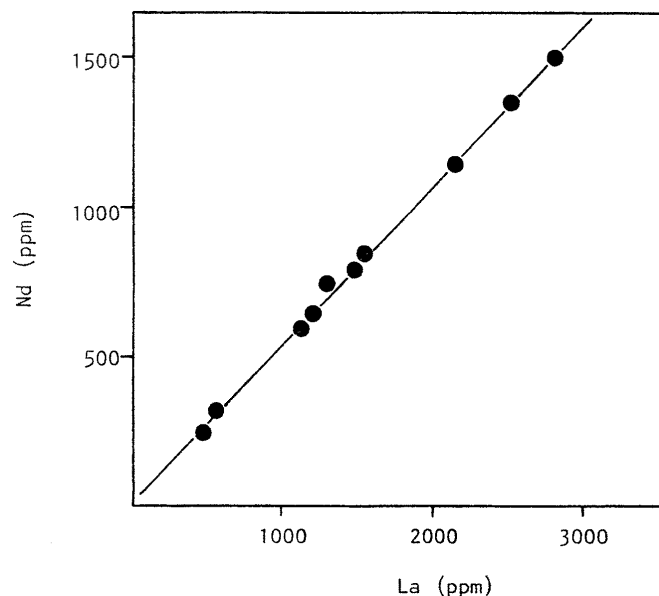
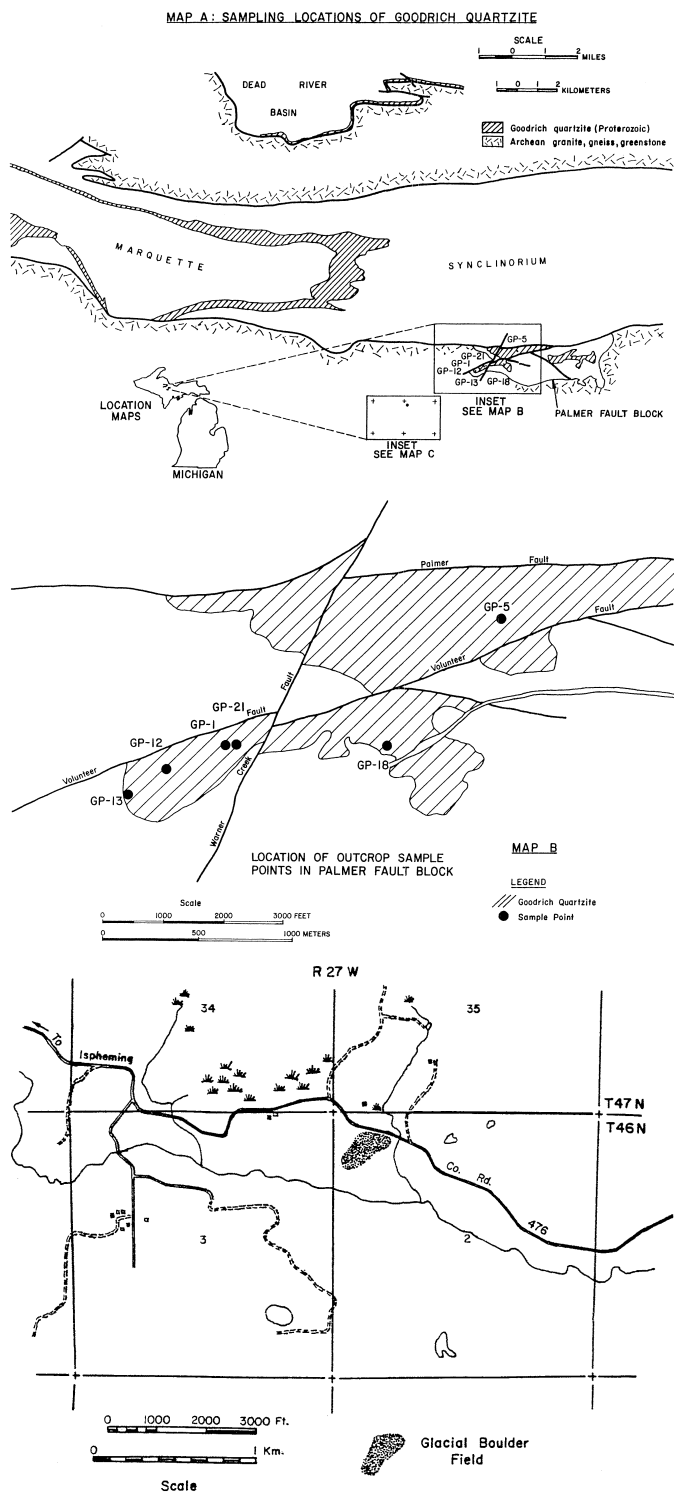


Figure 1. Nd vs. La, Goodrich quartzite. Correlation coefficient, $r = 0.9989$, the highest correlation coefficient found among all the possible pairs.

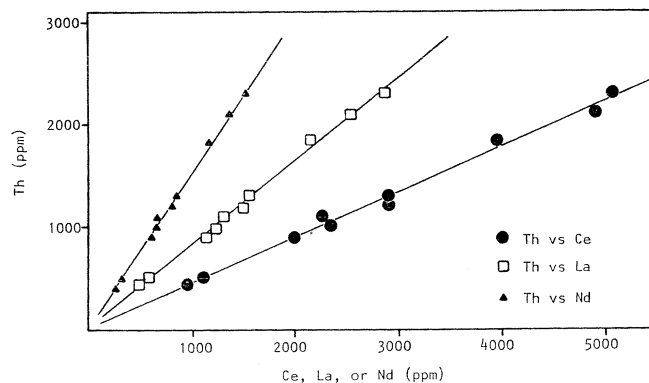


Figure 2. Th vs. Ce, Th vs. La, and Th vs. Nd, Goodrich quartzite. Correlation coefficients are 0.9947, 0.9986, and 0.9978 respectively.

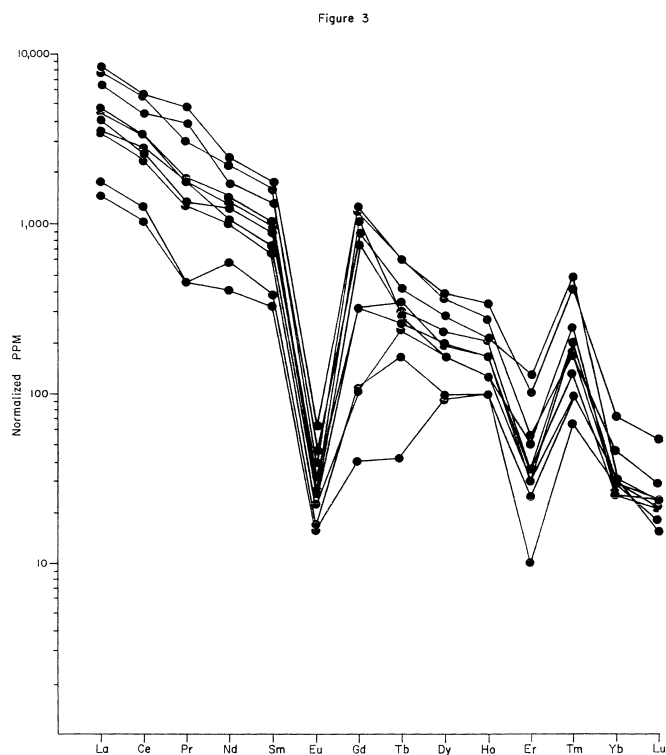


Figure 3. Normalized REE pattern for 10 Goodrich quartzite samples. Six are outcrop samples while four are glacial boulder samples.

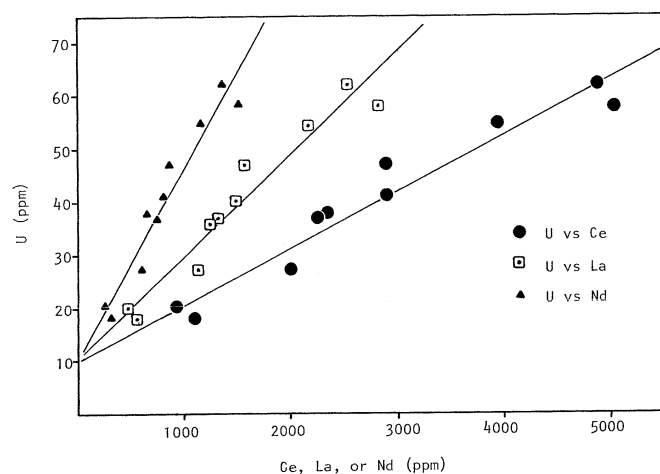


Figure 5. U vs. Ce, U vs. La, and U vs. Nd in the Goodrich quartzite from the Palmer fault block, Marquette County. Correlation coefficient for the three lines shown is 0.96. Six elements correlate with U with a correlation coefficient greater than 0.92. The intercepts for these regression lines range from 8.5 to 11.1 ppm U. The 10 ppm intercept most likely represents instrument background. Otherwise the 10 ppm U represents U not found in the mineral monazite.

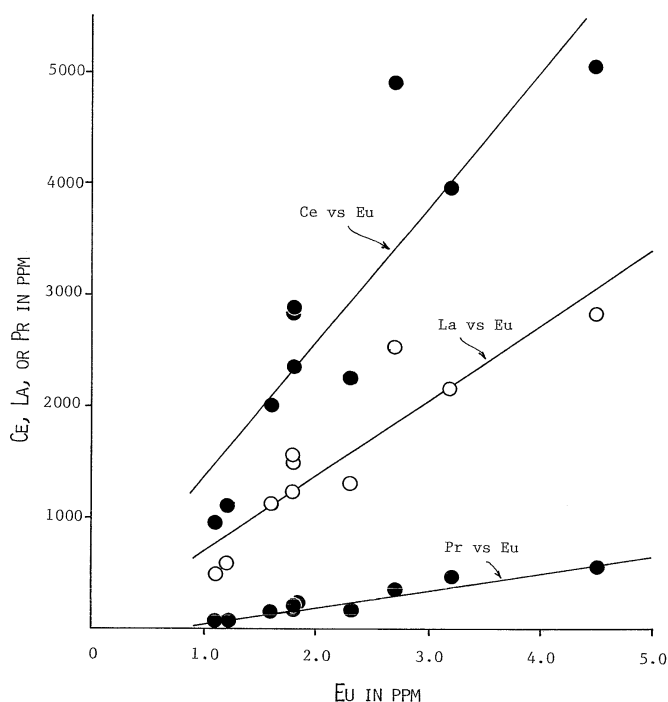


Figure 4. Ce vs. Eu, La vs. Eu, and Pr vs. Eu, Goodrich quartzite. Although Eu is depleted in the quartzite (see Figure 3), the fair to good correlations with Ce, La, and Pr indicate Eu abundance is controlled by monazite content.